COMPOSITION DEPENDENCE OF ELECTRICAL AND MAGNETIC PROPERTIES OF Ni–Ag THIS FILMS*

C. VAUTIER

Laboratoire d'Etude des Couches Minces Amorphes et Polycristallines, UFR Sciences et Techniques, B.P. 118, 76134 Mont-Saint-Aignan Cédex (France)

(Received May 31, 1988)

Summary

Ni–Ag thin films were prepared over the complete composition range by r.f. sputtering. The films are amorphous at room temperature in the composition range from 30 to 50 at.% Ag; they are ferromagnetic for compositions lower than 40 at.% Ag. Electrical resistivity, ordinary and extraordinary Hall coefficients as well as Curie temperature are studied.

1. Introduction

The phase diagram of Ni–Ag [1] shows a lack of miscibility even in the liquid state, except perhaps for low percentages where the phase diagram is poorly known. Thus it seemed very interesting to prepare Ni–Ag alloys by ways other than melt quenching. Moreover, most of the studied nickel-based alloys are of the transition metal–metalloid type [2]. Hauser [3] was the first to obtain Ni–Ag films in the composition range 32 - 61 at.% Ni by sputtering of sintered targets on cooled substrates; these films were amorphous. More recently, Munoz *et al.* [4] and Le Bas *et al.* [5] have obtained Ni–Ag films by co-evaporation but in a very narrow range of composition.

This paper deals with the study of Ni–Ag alloy thin films obtained by r.f. sputtering. We have determined the influence of composition on structure, resistivity and magnetic properties with a particular emphasis on the amorphous region.

2. Experimental details

The films are deposited by r.f. sputtering in a very pure argon atmosphere (99.9999% Ar) on substrates (freshly cleaved NaCl crystals or Vycor

*Paper presented at the Symposium on the Preparation and Properties of Metastable Alloys at the E-MRS Spring Meeting, Strasbourg, May 31 - June 2, 1988.

0022-5088/88/$3.50

glass) kept at a temperature of 88 K. For compositions up to 62 at.% Ag the target is made up of a nickel disk on which small silver squares of area 1 cm^2 are pasted, while for higher amounts of silver the target is made up of a silver disk with pasted nickel squares. The number of squares takes into account both the sputtering yields of the two components [6] and the desired composition (for more details on the preparation procedure see ref. 7 and references therein).

The sample composition is determined by measurement of the fluorescence line intensity of one of the elements [8]: the ratio of the intensity of a sample containing two elements to the intensity of a sample containing one element is proportional to the concentration of the element. The homogeneity of the films was tested by high resolution secondary ion mass spectrometry (SIMS) (CAMECA IMS 3F). Figure 1 shows nickel and silver profiles of a film containing 50 at.% Ag; we can see good homogeneity over the whole film thickness. Whatever the composition, even in the low percentage ranges [9], the samples are homogeneous.

The structure of the films was determined by electron diffraction: for compositions between 30 and 50 at.% Ag the diffraction patterns show the typical metallic glass aspect (Fig. 2(a)). For 50 at.% Ag a splitting of the second ring appears (Fig. 2(b)). For higher percentages (as well as for percentages lower than 30 at.% Ag) the films are microcrystalline (Figs. 2(c) and 2(d)).

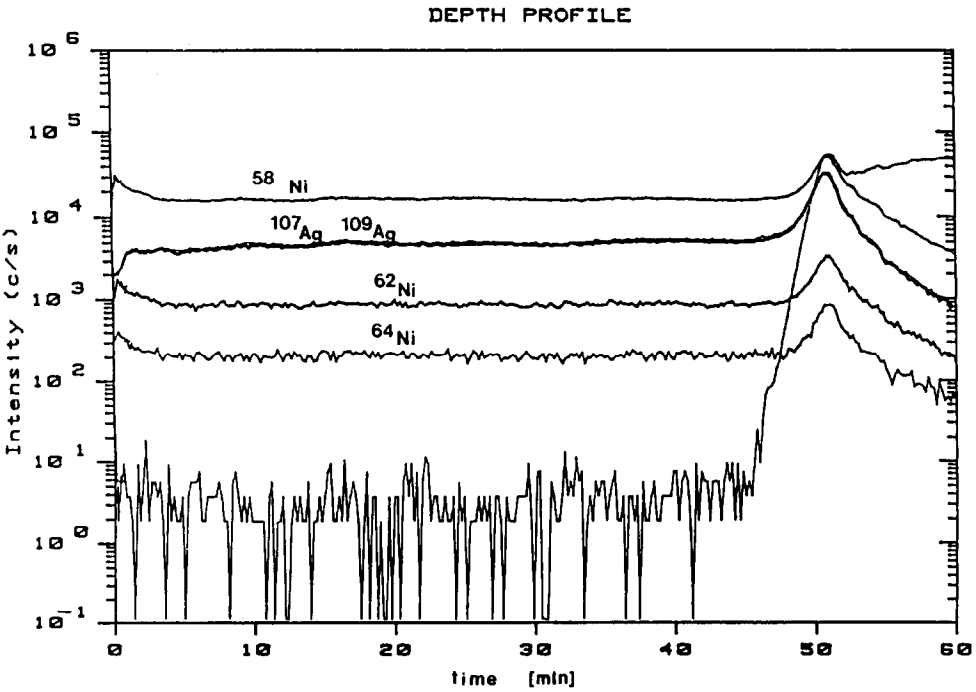

Fig. 1. SIMS nickel and silver profiles for a film containing 50 at.% Ag (the spectrum is normalized taking ^{58}Ni as the mass reference).

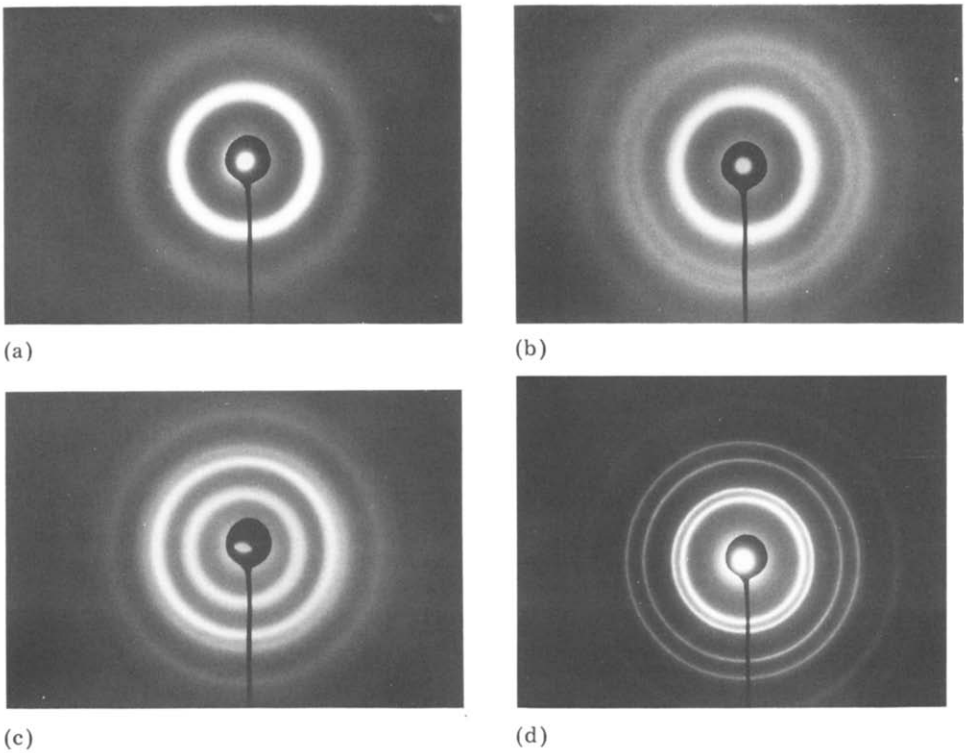

Fig. 2. Diffraction patterns for samples containing (a) 36 at.% Ag, (b) 50 at.% Ag and (c) 62 at.% Ag, and (d) a pure nickel film.

For resistivity and Hall effect measurements the Vycor substrates are provided with nickel electrodes of suitable shape. All the measurements are performed in a special device, the temperature of which may be regulated from 90 to 870 K within ±0.2 K [10].

3. Electrical properties

The resistivity is measured *in situ* between 88 and 600 K on thin films, the thickness of which is about 66 nm. The variation in the resistivity with temperature (Fig. 3) depends on the composition of the films. Curve 1 shows the behaviour of a pure nickel film which is typical for metallic films (except the slight decrease around 200 K (BC region), which is probably due to water desorption [7]). For microcrystallized films (curve 2) we observe a decrease in the BC region while the crystallization (EF zone) leads to a very low variation in the resistivity. Curve 3 shows a typical behaviour of amorphous films.

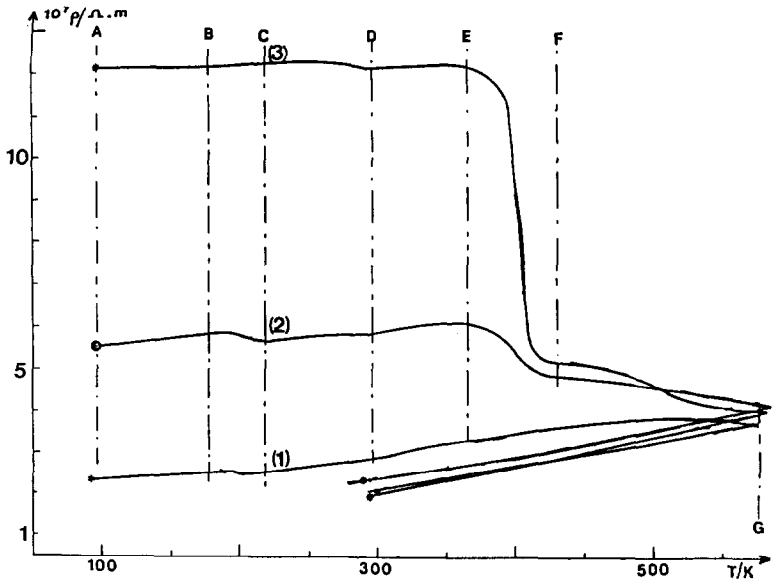

Fig. 3. Variation in resistivity with temperature: curve 1, pure nickel film; curve 2, microcrystalline film (10.5 at.% Ni); curve 3, amorphous film (39 at.% Ni).

(1) During annealing from 88 K to room temperature (A to D) the resistivity exhibits a low temperature coefficient.

(2) The amorphous-to-crystalline transformation occurs in a narrow temperature range (EF) between 360 and 400 K.

(3) A second transformation takes place at about 430 K; the decrease in resistivity may be due to the crystallization of another amorphous phase.

These last results are confirmed by differential scanning calorimetry. Indeed, the thermograms show two exothermic crystallization peaks at 134 and 157 °C. Moreover, these two phases have been characterized by X-ray diffraction [11].

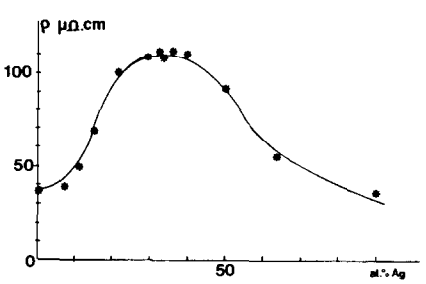

Fig. 4. Room temperature resistivity *vs.* composition of the films.

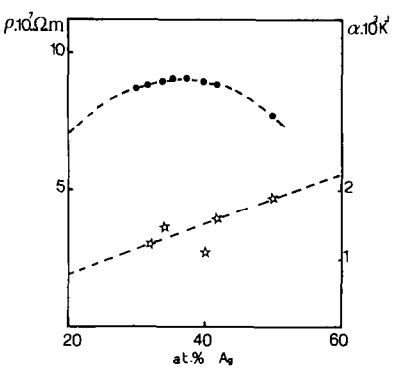

Fig. 5. Variation in resistivity and temperature coefficient with composition in the amorphous region.

The resistivity of the films at room temperature varies between 40 and 110 $\mu\Omega$ cm and has a maximum at about 35 at.% Ag (Fig. 4). We have reported on Fig. 5 the variation in temperature coefficient as well as resistivity variation with composition for amorphous samples; we can see that the temperature coefficient is always positive and, moreover, the resistivities are very similar in magnitude to those observed for liquid alloys, the shape of ρ *vs.* concentration curve is also similar [12]. Cote [13] was the first to explain the electrical resistivity behaviour in terms of Ziman theory for a liquid transition metal. Following Dreirach *et al.* [14], the electrical resistivity is given by

$$\rho = \frac{12\pi\Omega_0}{e^2\hbar {v_F}^2} \int_0^1 \mathrm{d}(q + 2k_F)\,(q + 2k_F)a(q)|t(q)|^2 \tag{1}$$

where $a(q)$ is the interference function, v_F the Fermi velocity, k_F the Fermi vector, Ω_0 the atomic volume and $|t(q)|$ a matrix which takes into account the scattering of electrons. It has been shown [14] that in the case of transition–noble metal alloys the resistivity may be written to a reasonable approximation as

$$\rho = \frac{30\pi^3\hbar^3}{me^2\Omega_0 {k_F}^2 E_F} \left|\sin^2\{\eta_2(E_F)\}\right| a(2k_F) \tag{2}$$

This formula shows the dependence of resistivity on both Fermi radius and phase shift η_2 which in the case of nickel is approximately 2.9 [15]. The comparison of the value k_p of k at the maximum of the interference function with k_F enables the determination of resistivity and temperature coefficient behaviour.

(1) If $2k_F < k_p$, the resistivity is low, its variation with composition exhibits a maximum and the temperature coefficient is positive.

(2) If $2k_F \approx k_p$, the resistivity exhibits a maximum but the temperature coefficient is negative.

(3) If $2k_F > k_p$, the resistivity varies linearly with composition.

Table 1 shows the values of k_p obtained from the interference functions and the values of $2k$F calculated by the relation [14]

$${k_F}^3 = \frac{3\pi^2(Z_{Ni}C_{Ni} + Z_{Ag}C_{Ag})}{\Omega_0} \tag{3}$$

where Z, the number of conduction electrons per atom, for nickel is taken to be equal to 0.6 and Z for silver equal to unity. The atomic volume is taken as a linear combination of the atomic volumes of the constituents:

$$\Omega_0 = C_{Ni}\Omega_{Ni} + C_{Ag}\Omega_{Ag} \tag{4}$$

Independent of the composition, the values of $2k_F$ are always lower than those of k_p, which gives a qualitative explanation of the variation with composition and of the positive temperature coefficient of resistivity.

TABLE 1

Fermi radius and maximum of interference function for amorphous samples

C_{Ag} (at.%)	$2k_F$ (Å^{-1})	k_p (Å^{-1})
32	2.633	2.88
36	2.638	2.89
40	2.639	2.90
44	2.641	2.93
50	2.644	2.96

4. Hall effect

The Hall effect is measured on thin films of 66 nm thickness. The magnetic induction may vary from 0 to 1 T and the temperature range is from 88 to 600 K. Figure 6 shows the variation in Hall voltage V_H *vs.* magnetic induction for films kept at 88 K. For alloys with less than 40 at.% Ag the $V_H(B)$ curves exhibit two linear parts, which is characteristic of ferromagnetic state. Above 40 at.% Ag the films are paramagnetic.

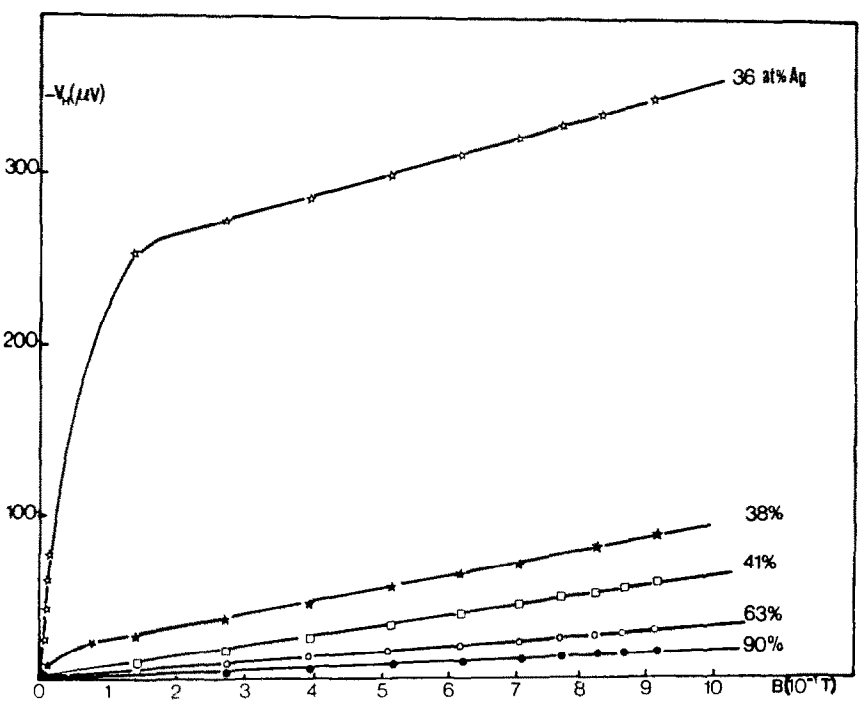

Fig. 6. Hall voltage *vs.* magnetic induction with silver concentration (atomic per cent) as parameter.

4.1. Ordinary Hall effect

In the ferromagnetic state it has been shown elsewhere [16] that the Hall resistivity may be written

$$\rho_H = \left| R_0 + (R_1 - R_0) \frac{\chi_S}{1 + \chi_S} \right| B + (R_1 - R_0) \frac{J_S}{1 + \chi_S}$$

where R_0 and R_1 are the "ordinary" and "anomalous" Hall constants respectively, J_S is the spontaneous magnetic polarization and χ_S is the saturation susceptibility. The slope of the linear part of $V_H = f(B)$ at high values of the magnetic induction permits the determination of the coefficient R_0' which is linked to R_0 by

$$R_0' = R_0 + (R_1 - R_0) \frac{\chi_S}{1 + \chi_S}$$

In the paramagnetic state the constant R_0' reduces to the ordinary Hall coefficient R_0. The variations in both Hall coefficients R_0' and R_0 with thin film composition are reported in Fig. 7. The striking feature is that in the paramagnetic state as well as in the ferromagnetic state the values of R_0 and R_0' do not depend on the structural state (amorphous or microcrystalline). We may then suppose that these coefficients depend only on local order and probably on the nickel atom environment. In the ferromagnetic region $R_0' = -2.6 \times 10^{-10}\ m^3\ C^{-1}$, a value greater than that obtained on thin nickel films ($-0.58 \times 10^{-10}\ m^3\ C^{-1}$) [16] but which closely resembles those obtained on amorphous Ni–Au alloys [17, 18].

In the paramagnetic region $R_0 = -0.8 \times 10^{-10}\ m^3\ C^{-1}$ whatever the composition, which means that the electron density and consequently the Fermi level remain constant. As in metals, one can derive from R_0 the effective number Z_{eff} of electrons per atom. In the case of an alloy this number is given by [18]

$$Z_{eff} = -\Omega_0 / eR_0$$

where Ω_0 is the mean atomic volume defined above. Figure 8 shows the variation in Z_{eff} with concentration (atomic per cent) of nickel; extrapolation to 100 at.% leads to the determination of the number of conduction electrons per atom, *i.e.* 0.6 in good agreement with the value found by Bergmann [18].

4.2. Anomalous Hall constant

In all the composition and temperature ranges where the samples are ferromagnetic R_1' is negative, which is consistent with the values observed in crystalline materials. The variation in R_1', measured at $T = 88$ K, with silver concentration (atomic per cent) is shown in Fig. 9; we observe a maximum for 30 at.% Ag which corresponds approximately to the maximum of resistivity.

4.3. Curie temperature

We have shown elsewhere [19] that the variation in R_0' with temperature enables the determination of the Curie temperature of the alloys. The variation in T_c with nickel content (Fig. 10) is linear with a slope of 7 K

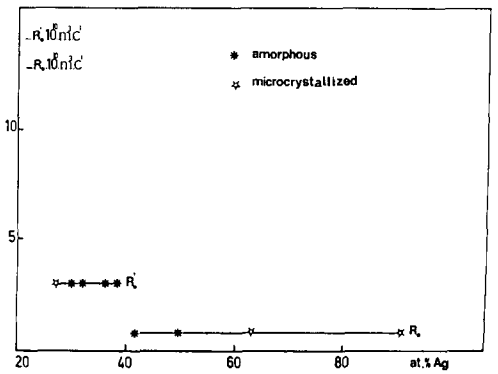

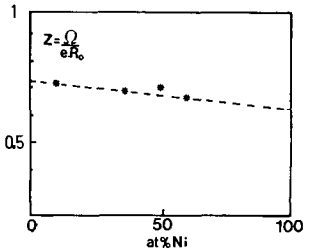

Fig. 7. Variation in ordinary Hall coefficients R_0 and R_0' with sample composition.

Fig. 8. Effective number of conduction electrons *vs.* nickel content.

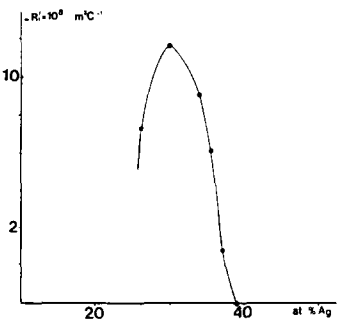

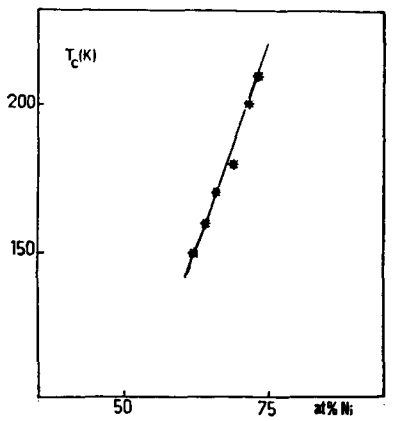

Fig. 9. Extraordinary Hall coefficient, measured at $T = 88$ K, *vs.* silver concentration (atomic per cent).

Fig. 10. Curie temperature *vs.* nickel content.

$(\text{at.}\%)^{-1}$ in good agreement with Hauser's results (9 K $(\text{at.}\%)^{-1}$) [3]. Extrapolation to $T_c = 0$ K gives the onset of ferromagnetism at a composition of 37 at.% in good agreement with experimental and Hauser's results. Extrapolation to 100 at.% Ni leads to $T_c = 440$ K for pure amorphous nickel, a result near that obtained by Hauser on amorphous nickel thin films deposited on cooled substrates (25 K) by getter sputtering [20]. At least we may notice that the Curie temperature is constant in the temperature range where the films remain amorphous.

5. Conclusion

It is possible to obtain Ni–Ag alloys over the entire composition range by r.f. sputtering on cooled substrates. Resistivity as well as extraordinary

Hall coefficient exhibit a maximum at around 30 at.% Ag which confirms that they are linked. The ordinary Hall coefficient is independent of the structural state in the paramagnetic as well as in the ferromagnetic region which means that it probably depends on local order.

References

1 M. Hansen and K. Andeko, *Constitution of Binary Alloys*, McGraw-Hill, New York, 1958, p. 36.
2 S. Takayama, *J. Mater. Sci., 11* (1976) 164.
3 J. J. Hauser, *Phys. Rev. B, 12* (1975) 5160.
4 A. Munoz, H. Miranda, F. L. Cumbrera, A. Conde and R. Marquez, *Thin Solid Films, 88* (1982) 211.
5 J. Le Bas, G. Richon, M. Bernole and M. Engel, *Société Française de Physique, Congr., Nice, 1985*, unpublished.
6 C. Sella, *Proc. 1st Symp. on Cathodic Sputtering, Toulouse, 1969*, p. 194.
7 L. Protin, J. Grenet and G. Fleury, *Rev. Phys. Appl., 21* (1986) 775.
8 J. Le Bas, E. Dittmar, L. Protin, D. Dubois, M. Bernole and R. Graf, *Thin Solid Films, 87* (1982) 195.
9 A. Tadjeddine, A. Benhabib, A. Zeghib and J. Le Bas, *J. Phys., 48* (1987) 715.
10 G. Lefrancois, L. Protin and D. Carles, *Vide, 209* (1981).
11 A. Chenoufi, *Thesis*, Rouen, 1988.
12 G. Busch, H. J. Guentherodt, H. U. Kuenzi, H. A. Meier and L, Schlafbach, *Mater. Res. Bull., 5* (1970) 567.
13 P. J. Cote, *Solid State Commun., 18* (1971) 1311.
14 O. Dreirach, R. Evans, H. J. Guntherodt and H. U. Kunzi, *J. Phys. F, 2* (1972) 709.
15 L. V. Meisel and P. J. Cote, *Phys. Rev. B, 15* (1977) 2970.
16 J. Le Bas, *Thin Solid Films, 10* (1972) 437.
17 G. Bergmann, *Solid State Commun., 18* (1976) 897.
18 G. Bergmann, *Z. Phys. B, 25* (1976) 255.
19 A. Zeghib, J. Le Bas and C. Vautier, *Phys. Status Solidi, 101* (1987) 487.
20 J. J. Hauser, *Phys. Rev. B, 17* (1968) 1908.